

<https://doi.org/10.1038/s42003-025-07607-w>

# Protein structure and interactions elucidated with in-cell NMR for different cell cycle phases and in 3D human tissue models

Check for updates

Jan Rynes<sup>1,8</sup>, Eva Istvankova<sup>1,8</sup>, Michaela Dzurov Krafcikova<sup>1,8</sup>, Enrico Luchinat<sup>2,3</sup>, Letizia Barbieri<sup>2</sup>, Lucia Banci<sup>2,3</sup>, Kristyna Kamarytova<sup>1</sup>, Tomas Loja<sup>1</sup>, Bohumil Fafilek<sup>4,5,6</sup>, Gustavo Rico-Llanos<sup>4,6</sup>, Pavel Krejci<sup>4,5,6</sup>, Libor Macurek<sup>7</sup>, Silvie Foldynova-Trantirkova<sup>1</sup>✉ & Lukas Trantirek<sup>1</sup>✉

Most of our knowledge of protein structure and function originates from experiments performed with purified proteins resuspended in dilute, buffered solutions. However, most proteins function in crowded intracellular environments with complex compositions. Significant efforts have been made to develop tools to study proteins in their native cellular settings. Among these tools, in-cell NMR spectroscopy has been the sole technique for characterizing proteins in the intracellular space of living cells at atomic resolution and physiological temperature. Nevertheless, due to technological constraints, in-cell NMR studies have been limited to asynchronous single-cell suspensions, precluding obtaining information on protein behavior in different cellular states. In this study, we present a methodology that allows for obtaining an atomically resolved NMR readout of protein structure and interactions in living human cells synchronized in specific cell cycle phases and within 3D models of human tissue. The described approach opens avenues for investigating how protein structure or drug recognition responds to cell-cell communication or changes in intracellular space composition during transitions among cell cycle phases.

Most of our knowledge of protein structure and function originates from experiments performed with purified proteins resuspended in dilute, buffered solutions. Under these *in vitro* (test-tube) conditions, the activities of proteins (enzymes) are sensitively modulated by the physicochemical factors in their surroundings, such as pH, ionic strength, or molecular crowding; the perturbations in these environmental factors translate into changes in the protein activities through alterations in their structures, stabilities, and/or dynamics over multiple time scales<sup>1–3</sup>.

However, most proteins carry out their function in intracellular environments that are crowded and of complex composition. By analogy to the *in vitro* settings, the physiological state-specific properties of the intracellular space tune proteins' activities/

properties *in vivo*<sup>4–8</sup>. Therefore, decoding intracellular environmental impacts on protein conformational behavior is vital for understanding and predicting phenotypes regarding protein activities in living human cells.

Major efforts have been made to develop tools for studying proteins in their native cellular settings, including cellular cryo-electron tomography, in-cell single-molecule Förster resonance energy transfer (FRET) spectroscopy, nuclear magnetic resonance (NMR) spectroscopy, and electron paramagnetic resonance (EPR) spectroscopy (reviewed in<sup>9</sup>). Among these tools, in-cell NMR spectroscopy is the sole technique for characterizing proteins in the intracellular space of living cells at atomic resolution and physiological temperature<sup>10,11</sup>.

<sup>1</sup>Central European Institute of Technology, Masaryk University, Brno, Czech Republic. <sup>2</sup>Interuniversity Consortium for Magnetic Resonance of Metallo Proteins, Sesto Fiorentino, Italy. <sup>3</sup>Magnetic Resonance Center and Department of Chemistry, University of Florence, Sesto Fiorentino, Italy. <sup>4</sup>Department of Biology, Faculty of Medicine, Masaryk University, Brno, Czech Republic. <sup>5</sup>Institute of Animal Physiology and Genetics, Czech Academy of Sciences, Brno, Czech Republic. <sup>6</sup>International Clinical Research Center, St. Anne's University Hospital, Brno, Czech Republic. <sup>7</sup>Institute of Molecular Genetics, Czech Academy of Sciences, Prague, Czech Republic. <sup>8</sup>These authors contributed equally: Jan Rynes, Eva Istvankova, Michaela Dzurov Krafcikova. ✉e-mail: [silvie.trantirkova@ceitec.muni.cz](mailto:silvie.trantirkova@ceitec.muni.cz); [lukas.trantirek@ceitec.muni.cz](mailto:lukas.trantirek@ceitec.muni.cz)

The success of in-cell NMR applications critically relies on the ability to deliberately increase the concentration of the protein(s) of interest within the cell's interior. This increase, usually accompanied by isotopic labeling, allows for separating NMR signals linked to the target protein from those originating from other cellular components<sup>11</sup>. This elevated protein concentration is achieved by introducing the recombinant protein from outside the cells<sup>4,6,12,13</sup> or in situ transient protein overexpression<sup>14</sup>. However, these methods are intrusive, stochastic, and/or require specific cell culture manipulations, making it problematic to achieve uniform protein levels in the intracellular space and maintain precise control over their physiological state during in-cell NMR experiments conducted at 37 °C.

Thus far, the applications of in-cell NMR spectroscopy to study proteins in living human cells have remained confined to so-called asynchronous single-cell suspensions (reviewed in<sup>11</sup>), which are mixtures of cells in distinct phases of the cell cycle. Although every cell cycle phase is marked by a unique composition and physicochemical properties of the intracellular space<sup>15–17</sup>, the in-cell NMR spectra acquired on asynchronous single-cell suspensions report only an ensemble average NMR signal across the population of cells in the active volume of the NMR coil; the information about the cell cycle phase-specific impact of intracellular space properties on protein structure is lost making interpretation of resulting in-cell NMR data in physiological terms challenging.

We hypothesized that the inducible overexpression of a protein target from chromosomal loci could enable control over the cell synchronicity of cells during NMR data acquisition. In this study, we investigated the feasibility of preparing in-cell NMR samples of proteins from inducible, stably transfected cell lines. We demonstrate that the inducible overexpression of the protein target in stably transfected cells allows for simultaneous control over isotopic labeling and chemically induced cell cycle phase synchronization. We illustrate that isolating and expanding a single clone from the polyclonal inducible stable cell line is instrumental for achieving uniform protein overexpression levels across the cell population included in the in-cell NMR sample and the sensitivity required to obtain high-resolution in-cell NMR spectra of a target protein not only in specific cell cycle phases but also in a model of human tissue. Applying the presented method can provide unique information on protein behavior under various physiological situations, *i.e.*, information currently inaccessible to other biophysical tools.

## Results

To scrutinize the hypothesis, we initially employed the PiggyBac (PB) Cumate Switch Inducible Vector (System Biosciences, US) (Supplementary Fig. 1A) for several reasons: (i) The TTAA-specific transposon piggyBac is rapidly becoming a highly useful vector for genetic engineering of a wide variety of species, comprising insects, yeast, and mammals, including humans<sup>7</sup>; (ii) it allows inducible protein overexpression under the control of the cumate operator; the inducibility of protein expression is essential for the cell's physiological state and protein isotopic labeling control; (iii) it allows for the insertion of multiple copies of the gene of interest at various genomic locations; it might be vital for achieving the protein overexpression levels required for NMR detection; and (iv) it contains a gene coding for green fluorescent protein (GFP) under the control of an internal ribosomal entry site (IRES) following the stop codon of the target protein, which facilitates indirect monitoring of target protein expression via GFP fluorescence while not affecting the target protein in-cell NMR readout (GFP resonances are too broad to be observed in cells, most likely due to interactions with intracellular components, decreasing its rotational diffusion rate<sup>18,19</sup>).

We inserted the human superoxide dismutase 1 (hSOD1) gene into the PB Cumate Switch Inducible Vector (Fig. S2A), generating a stable HEK293T cell line (HEK293T<sup>CuR-hSOD1/Poly</sup>). Upon cumate exposure, hSOD1 expression in HEK293T<sup>CuR-hSOD1+/Poly</sup> cells monitored indirectly via a GFP reporter was low (Supplementary Figs. 1B and 3A) and insufficient for NMR readout.

To enhance expression, we replaced the cumate operator (CuO) and repressor (CuR) with the tetracycline operator (TetO) and repressor (TetRep; TR) (Supplementary Fig. 2B). A stable cell line generated using this

modified vector expressed hSOD1 at increased levels in the presence of tetracycline; however, hSOD1 expression leaked in the absence of tetracycline (Supplementary Figs. 1C and 3B).

To suppress leakage of target protein expression, we integrated the modified vector into a cell line stably expressing the tetracycline repressor Flp-In T-Rex 293 (HEK293-TREx) (Fig. 1A); hSOD1 expression in the resulting polyclonal cell line (HEK293-TREx<sup>TR-hSOD1+/Poly</sup>) was rigorously controlled with tetracycline (Fig. 1B, C and Supplementary Fig. 3C), with levels resembling those in HEK293T cells (Supplementary Figs. 1C and 3B). Moderate differences in the hSOD1 expression levels, as revealed via the GFP reporter, were observed among cells in the polyclonal culture (Fig. 1B, C and Supplementary Fig. 3C), likely stemming from differences in the number of gene copies and the genomic integration sites. Nevertheless, the differences were much lower than those typically encountered when using transient transfection (Supplementary Figs. 4A, B).

To improve the uniformity of protein expression, a crucial factor for reliably interpreting in-cell NMR experiments, we isolated high-expression clones from HEK293-TREx<sup>TR-hSOD1+/Poly</sup> cells based on the GFP reporter intensity. The expansion of these clones yielded monoclonal cell lines (HEK293-TREx<sup>TR-hSOD1/Mono</sup>), which displayed higher and more uniform hSOD1 expression levels than did HEK293-TREx<sup>TR-hSOD1+/Poly</sup> (Fig. 1B, C and Supplementary Fig. 3C vs. Supplementary Fig. 3D). Acquired 2D <sup>1</sup>H-<sup>15</sup>N SOFAST-HMQC in-cell NMR spectrum of hSOD1 in induced monoclonal stably transfected (HEK293-TREx<sup>TR-hSOD1+/Mono</sup>) cells demonstrated that this strategy is suitable for acquiring in-cell NMR data (Fig. 1D, E and Supplementary Fig. 5A, B). The procedure was successfully validated for two additional model proteins: the small bacterial protein TTHA (HEK293-TREx<sup>TR-TTHA+/Mono</sup>—Fig. 2A, Supplementary Fig. 6A, C) and human carbonic anhydrase II (hCAII) (HEK293-TREx<sup>TR-hCAII+/Mono</sup>—Fig. 2B, Supplementary Fig. 6B and D). The analysis of western blot data acquired from lysates of cells used for in-cell NMR samples indicated that the intracellular concentrations of target proteins were in the range of 20–70 μM (Supplementary Fig. 7). This estimate suggests that the achievable intracellular target protein concentrations using our system are lower than those attainable with the transient transfection approach<sup>20</sup>.

To assess the possibility of achieving in-cell NMR readout in cell cycle phase synchronized (HEK293-TREx<sup>TR-hCAII+/Mono</sup>) cells, we induced protein overexpression for 48 h while subjecting the cell culture to 14 and 24 h of mimosine or RO3306 and nocodazole treatment for G<sub>1</sub>/S and G<sub>2</sub>/M-phase synchronization<sup>21–23</sup>, respectively (Fig. 3). To maintain cell viability and synchronization during prolonged in-cell NMR spectra acquisition, we continuously supplied fresh medium supplemented with mimosine and nocodazole to G<sub>1</sub>/S and G<sub>2</sub>-phase synchronized cells, respectively, using an NMR bioreactor<sup>24</sup>. Nocodazole treatment of G<sub>2</sub>-phase synchronized cells was employed to prevent potential completion of mitosis during the measurement, trapping cells at G<sub>2</sub>/M. The resulting in-cell NMR spectra of CAII in G<sub>1</sub>/S- and G<sub>2</sub>/M-phase synchronized cells exhibited the expected signals from Zn<sup>2+</sup>-coordinated His residues in the CAII active site<sup>25</sup> in the region between 11.0 and 15.5 ppm; the spectra showed comparable S/N ratios and resolutions and did not exhibit substantial differences, consistent with the housekeeping role of CAII (Fig. 3A<sub>3</sub>, B<sub>3</sub>). Upon adding methazolamide (MZA), a validated CAII inhibitor, both spectral patterns changed and matched the previously reported spectrum of the CAII-MZA-bound state<sup>25</sup> (Fig. 3A<sub>3</sub>, B<sub>3</sub>). These data demonstrated the capacity of in-cell NMR to assess protein structure and interactions with drug-like molecules in different cell cycle phases.

Notably, acquiring the capacity to record in-cell NMR data in stably transfected cells has opened the possibility of extending the in-cell NMR concept to 3D cell cultures<sup>26</sup>, which is a crucial milestone for high-resolution NMR protein studies in tissues/organs. 3D cell cultures, particularly hybrid preparations consisting of different cell types, allow more physiological in vitro modeling of cell metabolism and cell-matrix and cell-to-cell interactions than traditional 2D single-cell cultures<sup>27</sup>.

To assess this possibility, we separately used HEK293-TREx<sup>TR-TTHA+/Mono</sup> and HEK293-TREx<sup>TR-hCAII+/Mono</sup> cells to form spheroids, primitive human

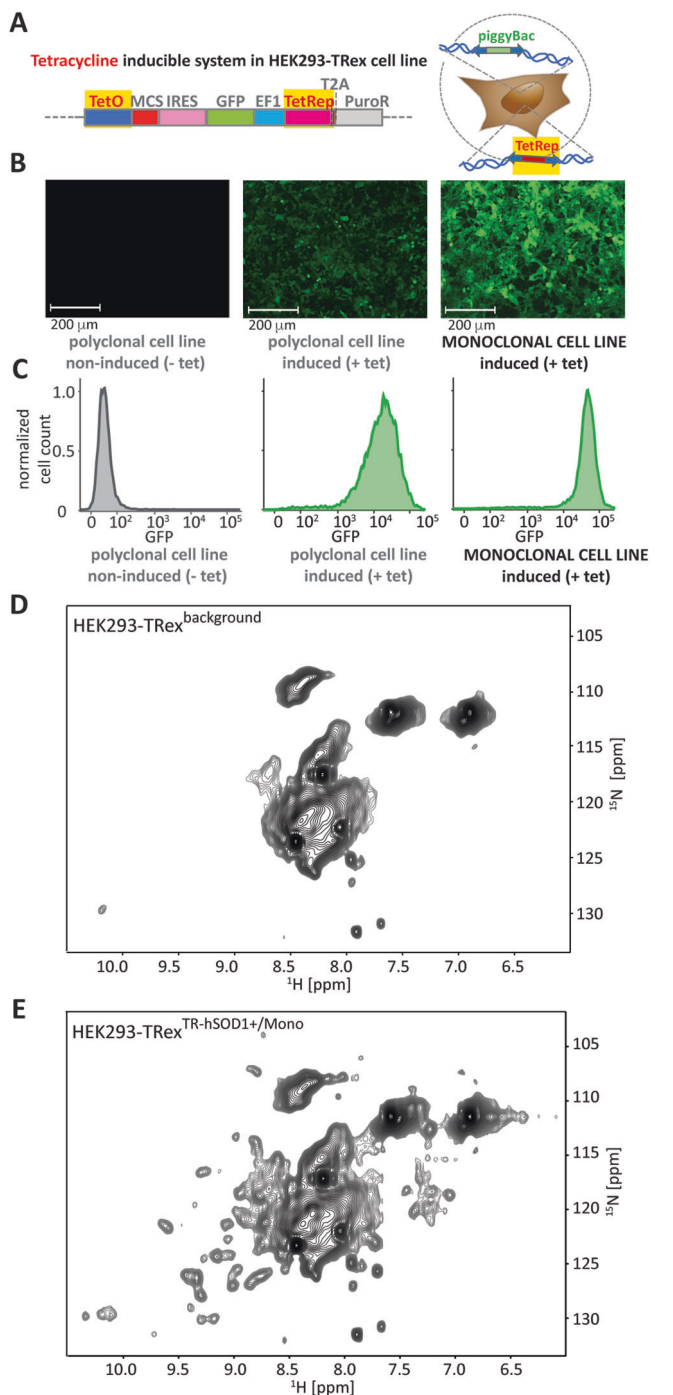


**Fig. 1 | Tetracycline-inducible expression in mono-clonal cell lines is sufficient for the acquisition of target protein in-cell NMR spectra.** **A** Scheme of the tetracycline-inducible piggyBac construct inserted into HEK293-Trex cells. **B** Confocal images showing the GFP reporter expression in non-induced HEK293-Trex<sup>TR-hSOD1+/Poly</sup> cells (control) and HEK293-Trex<sup>TR-hSOD1+/Poly</sup> and HEK293-Trex<sup>TR-hSOD1+/Mono</sup> cells induced with tetracycline for 48 h. **C** Flow cytometry (FCM) plots for non-induced HEK293-Trex<sup>TR-hSOD1+/Poly</sup> cells, and HEK293-Trex<sup>TR-hSOD1+/Poly</sup> and HEK293-Trex<sup>TR-hSOD1+/Mono</sup> cells 48 h after expression induction. **D, E** <sup>1</sup>H-<sup>15</sup>N 2D SOFAST-HMQC in-cell NMR spectra of (pelleted) non-induced HEK293-Trex<sup>TR-hSOD1+/Mono</sup> cells (background) and HEK293-Trex<sup>TR-hSOD1+/Mono</sup> cells 48 h after induction, respectively.

tissue models. Spheroid formation and protein expression occurred simultaneously over 48 h, resulting in spheroids <250 μm in size (Fig. 4A1 and Supplementary Fig. 4C–E). Before NMR data acquisition, the spheroids were immobilized in a gel matrix to facilitate bioreactor-assisted measurements and prevent their fusion.

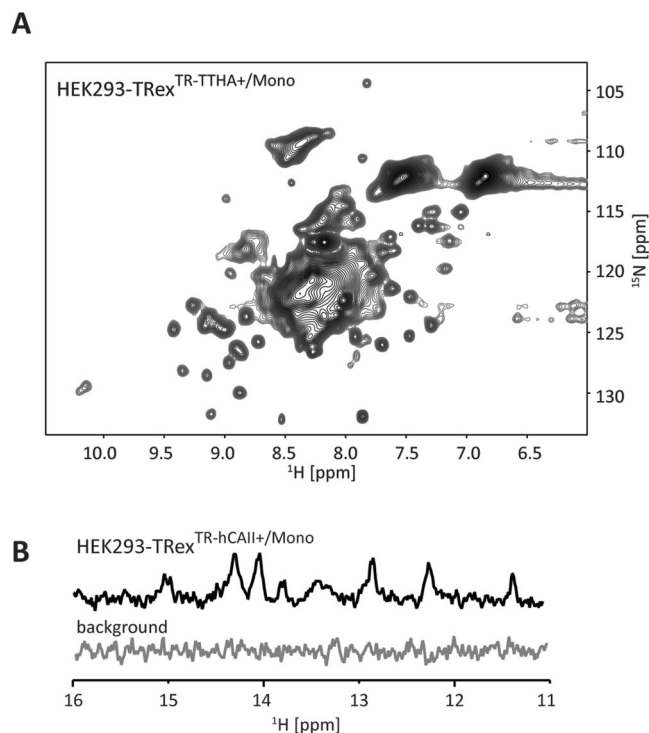


**Fig. 2 | The application of stable cell line approach for preparation of in-cell NMR samples of TTHA and CAII.** **A** <sup>1</sup>H-<sup>15</sup>N 2D SOFAST-HMQC in-cell NMR spectra from HEK293-Trex<sup>TR-TTHA+/Mono</sup> cells, 48 h after expression induction. **B** The imino regions of <sup>1</sup>H 1D in-cell NMR spectra of induced and non-induced (background) HEK293-Trex<sup>TR-hCAII+/Mono</sup> cells. NMR spectra were measured at 37 °C using a bioreactor.

The resulting NMR spectra of spheroid-based samples from HEK293-Trex<sup>TR-TTHA+/Mono</sup> and HEK293-Trex<sup>TR-hCAII+/Mono</sup> cells exhibited the expected patterns. They demonstrated comparable signal-to-noise ratio (S/N ratio) and resolution to those obtained from the corresponding single-cell suspensions (Fig. 4A<sub>3</sub>, A<sub>4</sub>). Notably, the introduction of MZA to the medium supplied to HEK293-Trex<sup>TR-hCAII+/Mono</sup>-based spheroids induced a change in the spectral pattern within the 11.0 to 15.5 ppm region, corresponding to the spectrum of the CAII-MZA-bound state (Fig. 4A<sub>4</sub>—red) and confirming a possibility to conduct in-cell NMR-based drug screening in 3D tissue culture systems.

To assess the possibility of conducting in-cell NMR studies in hybrid 3D cultures, we embedded the HEK293-Trex<sup>TR-hCAII+/Mono</sup> spheroids in a gel matrix containing MCF7 cells (Fig. 4B), which exhibit an epithelial-like morphology<sup>28</sup>. For visualization, we used MCF7 cells stably transfected with the pKrox24 reporter (MCF7<sup>pKrox24DsRED</sup>), which expresses destabilized red fluorescent protein (DsRED), upon treatment with fibroblast growth factor 2 (FGF2). In this way, we created the simplest model mimicking a complex organ, where 3D spheroids were surrounded by cells of different types, referred to as HEK293-Trex<sup>TR-hCAII+/Mono</sup>::MCF7<sup>pKrox24DsRED</sup> spheroids. The comparison of the imino region of the 1D <sup>1</sup>H in-cell NMR spectra of the HEK293-Trex<sup>TR-hCAII+/Mono</sup> and HEK293-Trex<sup>TR-hCAII+/Mono</sup>::MCF7<sup>pKrox24DsRED</sup> spheroids before and after treatment with the CAII inhibitor (MZA) (Fig. 4A<sub>4</sub>, B<sub>3</sub>) demonstrated the potential for conducting in-cell NMR-based drug screening also in hybrid 3D tissue culture systems.

## Discussion

We adapted the PB transposon system to allow the insertion of a gene of interest under the control of the tetracycline operon into the genome of human cells stably transfected with a tetracycline repressor. We demonstrated that inducing the overexpression of the target protein in the resulting mono-clonal stably transfected cell line enables isotopic labeling control and

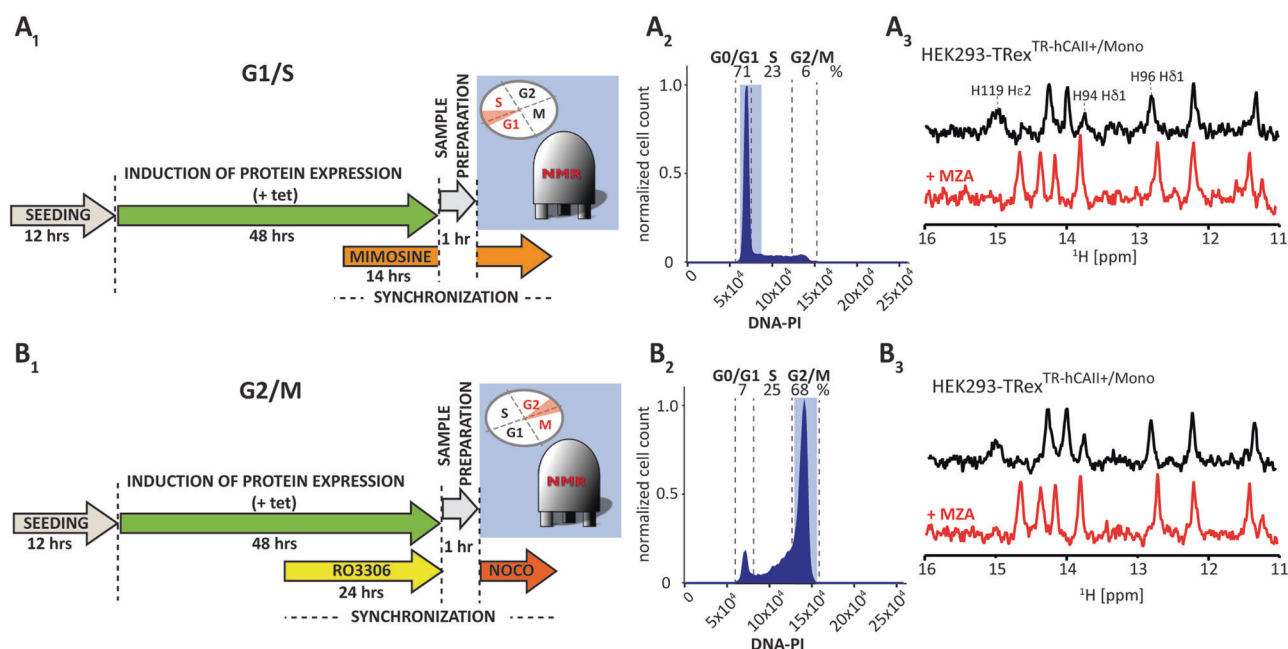


**Fig. 3 | The stably transfected cell lines allow the acquisition of in-cell NMR spectra in distinct cell cycle phases.** **A**, **B** Overview of the stable cell line manipulations leading to the acquisition of in-cell NMR spectra (**A**<sub>1</sub>) at the G<sub>1</sub>/S and (**B**<sub>1</sub>) G<sub>2</sub>/M boundary of the cell cycle. The propidium iodide (PI) DNA content staining of G<sub>1</sub>/S (**A**<sub>2</sub>) and G<sub>2</sub>/M (**B**<sub>2</sub>) synchronized HEK293-TRex<sup>TR-hCAII+/Mono</sup> cells before gel

immobilization and NMR analysis, <sup>1</sup>H 1D in-cell NMR spectra of G<sub>1</sub>/S (**A**<sub>3</sub>) and G<sub>2</sub>/M (**B**<sub>3</sub>) synchronized HEK293-TRex<sup>TR-hCAII+/Mono</sup> cells 48 h after expression induction before (black) and after (red) addition of MZA. Signals arising from the zinc-coordinating histidines (H94, H96, and H119) in the active site of CAII are indicated. NMR spectra were measured at 37 °C using a bioreactor.

results in uniform intracellular protein levels adequate for obtaining in-cell NMR spectra of the protein. Importantly, we showed that utilizing the inducible monoclonal stably transfected cell lines provides a crucial advantage in accessing atomically resolved information on protein structure in individual phases of the cell cycle and 3D cell cultures. The procedure is compatible with multiple isotopic labeling schemes in living human cells, including the recently introduced schemes for protein labeling with unnatural amino acids tailored for drug screening applications<sup>29</sup>.

Based on Western blot data acquired from lysates of cells used for in-cell NMR samples, we estimated the intracellular concentrations of target proteins to be in the range of ~20–70 μM. This is comparable to the typical concentration achieved with electroporation but lower than the concentration achievable with transient transfection approaches (~350 μM)<sup>11,14,20</sup>. On the one hand, these concentrations are too low to determine protein structure in mammalian cells using currently available NMR hardware and labeling schemes. On the other hand, these concentrations are still higher than endogenous protein levels, which are typically around 1 μM. When drawing conclusions from in-cell NMR studies, it is thus essential to consider that high concentrations of overexpressed target proteins can saturate the pool of native binding partners. In such cases, the observed NMR signals primarily originate from a pool of freely tumbling protein targets. Consequently, the information derived from in-cell NMR data on cells with elevated (non-native) target protein levels does not necessarily reflect the target's functional biology but instead the effects of the complex cellular environment on its structural behavior.

Noteworthy, the information regarding intracellular protein target levels obtained from our system must be interpreted in the context of the monoclonal selection step. The monoclonal cell lines used in this study were deliberately expanded from isolated clones exhibiting the highest target protein expression levels. Thus, the estimated intracellular protein concentrations should be considered only an upper limit achievable with our system. Employing cell sorting to isolate clones with lower intracellular protein levels offers an effective way of controlling intracellular target concentration to align with available NMR hardware and labeling and acquisition schemes.

The capacity of the presented method to deliver information on protein conformation in cell cycle phase-synchronized cells can be regarded as an alternative to the recently introduced “pre-synchronization” concept for nucleic acids by Viskova et al.<sup>30</sup>. The authors of that study demonstrated the possibility of acquiring in-cell NMR data on nucleic acid fragments delivered via electroporation into HeLa cells pre-synchronized in distinct cell cycle phases. Considering that electroporation was initially used to prepare protein in-cell NMR samples from asynchronous cells<sup>6</sup>, it is conceivable that Viskova et al.'s<sup>30</sup> method could be extended to proteins.

However, each method has specific limitations and application potential for in-cell NMR studies of proteins in cell cycle phase-synchronized cells. One significant advantage of the electroporation-based approach is its versatility concerning cell types. The electroporation method for structured and unstructured proteins has been demonstrated in several human cell lines, such as HeLa and others<sup>6,31–33</sup>. In contrast, the method presented here is currently limited to HEK293 cells and potentially a few other cell types capable of expressing target protein levels sufficient for detecting in-cell NMR protein signals using currently available NMR hardware and acquisition schemes. The expression from the PiggyBac-based construct utilized in this study is driven by the cytomegalovirus (CMV) promoter, which exhibits the highest activity in HEK293 cells<sup>34</sup>. Consequently, applying our construct to other cellular models may not yield the intracellular protein concentrations required to detect NMR signals; replacing the CMV promoter with alternative promoters may be necessary to achieve the desired target protein expression levels in different cell types.

Additionally, the electroporation-based approach enables the delivery of exogenously produced protein targets into cells. These targets can be isotopically labeled (with <sup>13</sup>C or <sup>15</sup>N) or chemically modified, such as fluorophores, spin labels, or non-native NMR-active nuclei such as <sup>19</sup>F. This capability allows for efficient separation of the spectral information from the target protein from the cellular background. In contrast, the stable-transfection approach introduced here relies on the overexpression of a (typically) isotopically labeled protein target in cells grown in an isotopically labeled medium. In this case, the in-cell NMR spectra of the overexpressed protein are inherently contaminated with the spectral background from

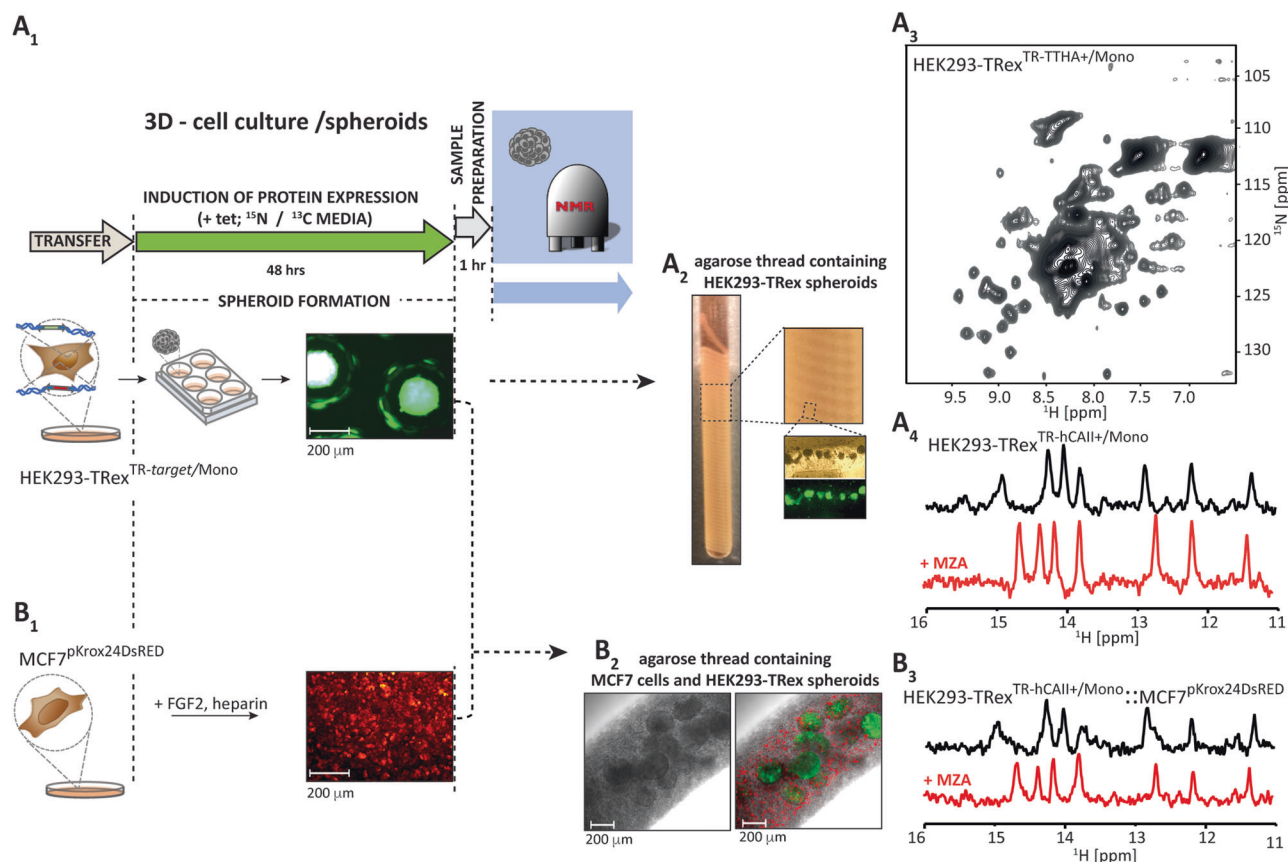


**Fig. 4 | The stable cell lines allow the acquisition of in-cell NMR spectra from 3D models of human tissue. A<sub>1</sub>, B<sub>1</sub>** Overview of the stable cell line manipulations leading to the acquisition of in-cell NMR spectra in 3D cell culture (spheroids); (A<sub>2</sub>) (Microscope) images of the in-cell NMR sample consisting of HEK293-TRex<sup>TR-TTHA+/Mono</sup> spheroids (green) embedded in low-melting agarose gel thread; (B<sub>2</sub>) (Microscope) images of the hybrid in-cell NMR sample consisting of MCF7<sup>pKrox24DsRED</sup> cells (red; DsRED expression induced by addition of FGF2)

and HEK293-TRex<sup>TR-hCAII+/Mono</sup> spheroids (green) embedded in low-melting agarose gel thread; (A<sub>3</sub>) <sup>1</sup>H-<sup>15</sup>N 2D SOFAST-HMQC in-cell NMR spectrum of spheroid preparation from induced HEK293-TRex<sup>TR-TTHA+/Mono</sup> cells; (A<sub>4</sub>) <sup>1</sup>H 1D in-cell NMR spectra of HEK293-TRex<sup>TR-hCAII+/Mono</sup> and (B<sub>3</sub>) HEK293-TRex<sup>TR-hCAII+/Mono</sup>::MCF7<sup>pKrox24DsRED</sup> spheroids before and after treatment with 100 μM CAII inhibitor MZA. NMR spectra were measured at 37 °C using a bioreactor.

isotopically labeled components of the cells, which interferes with the observation of many protein signals, particularly for intrinsically disordered proteins.

For these reasons, Viskova's<sup>30</sup> method could be preferable for preparing in-cell NMR samples of intrinsically disordered proteins and samples for solid-state in-cell NMR, with the inherent advantage of allowing for the employing of complementary techniques such as in-cell EPR and in-cell FRET spectroscopy, both of which require chemical modifications of the protein target.

On the other hand, using the presented method for in-cell NMR studies in cell cycle phase-synchronized cells can be considered an alternative to Viskova's<sup>30</sup> approach for structured/folded proteins whose structural integrity would be irreversibly affected by heat generated during the electroporation step (cf.<sup>35</sup>), or whose structural behavior in cells would be biased due to their origin (e.g., expression in a bacterial host) and in vitro manipulations: the stable-transfection approach provides the advantage of investigating targets that are produced, folded, and matured in situ. Moreover, the non-invasiveness of the presented method might be crucial for achieving cell cycle phase-resolved readouts. Perturbation of cell membrane integrity during protein electroporation inherently affects cell fitness and ultimately leads to increased mortality among transfected cells. Nonetheless, as demonstrated for electroporated asynchronous mammalian cell suspensions<sup>6</sup>, the issue of compromised cell fitness due to electroporation can be effectively addressed by incorporating a several-hour period between electroporation and in-cell NMR sample assembly. During this time, the electroporated cells can recover under optimal growth conditions.

Subsequently, metabolically active (viable) cells are separated from dead cells and those with compromised fitness, typically based on the inability of the latter to adhere to surfaces. However, maintaining cell cycle phase synchronicity among electroporated cells requires exposing them to chemicals (synchronization signals) during recovery and in-cell NMR spectrum acquisitions to prevent cell cycle resumption. It is currently unknown how cells electroporated with proteins respond to synchronization signals and whether their synchronicity can be maintained at physiological temperature for an extended period.

In contrast, the issue of perturbed cell fitness does not apply to stably transfected cells. As demonstrated here, the synchronicity of cell suspensions can be maintained for at least 9 h, which is compatible with the time requirements of most heteronuclear NMR acquisition schemes commonly used for in-cell NMR measurements on isotopically labeled proteins. Conceivably, the method presented can be considered for unstable protein targets that are rapidly degraded inside cells or when the studied phenomena require access to heteronuclear NMR data (which involves prolonged acquisition times), a minimally perturbed cellular environment, physiological temperature, and highly uniform protein levels across cell suspension. These situations might include real-time monitoring of processes such as drug binding thermodynamics/kinetics and studies of intrinsic protein dynamics using relaxation NMR methods, arguably constituting the main future challenge in protein in-cell NMR.

The method described is currently the only option for in-cell NMR studies in 3D cell cultures. Future advancements—such as the development of next-generation NMR spectrometers operating at magnetic fields of up to

35 T, along with improvements in NMR methodologies and isotopic labeling techniques—are expected to enhance sensitivity<sup>36</sup> and broaden the applications of the method for protein-in-cell NMR studies in complex models of human tissues, such as organoids, whose production implicitly requires stable transfection of the genomes of embryonic stem cells.

Conceivably, the in-cell NMR data from cell cycle phase-synchronized cells and the 3D models of human tissue have the potential to act as a unique source of information on protein behavior that is currently unattainable with other biophysical tools.

## Methods

### Vector construction

The inducible PiggyBac Cumate Switch vector (pB-CuRep), along with the Super PiggyBac Transposase expressing vector (pB-Transp), were purchased from System Biosciences. The pB-CuRep vector contains the cumate switch combined with the EF1-CymR repressor-T2A-Puro cassette. The expression of the cDNA of interest, inserted into the multi-cloning site (MCS) downstream of the cumate operator (CuO), can be switched on by adding cumate to the cells. Several cloning steps reconstructed the pB-CuRep vector from a cumate inducible vector to a vector inducible by tetracycline (pB-TetRep). The CuO was replaced by the tetracycline operator (TetO), and a fragment of the cumate repressor (CuRep; CuR) was replaced by the tetracycline repressor (TetRep; TR). cDNA of human SOD1 (hSOD1) bearing the sequence coding flag-tag (DYKDDDDK) on the 3' end was inserted into MCS of pB-CuRep. cDNAs of human SOD1 (hSOD1), CAII (hCAII), and bacterial TTHA1718 (TTHA) genes, bearing in all cases the sequence coding flag-tag on the 3' end, were individually inserted into MCS of pB-TetRep. Note: Introducing the C-terminal flag-tag to wild-type proteins aimed to facilitate the monitoring of hSOD1, TTHA, and hCAII expression levels using flag-tag specific antibodies (Sigma Aldrich, F1804) relative to the expression levels of the GFP reporter (cf. Figs. S5 and S6).

### Cell lines and cell cultivation

The HEK293T cell line (ATCC, CRL-3216) and the Flp-In T-REx 293 cell line (ThermoFisher) were employed to establish stable, inducible cell lines for in-cell NMR studies. Non-transfected HEK293T cells and HEK293T transfected with pB-CuRep (Merck) were cultured in Dulbecco's Modified Eagle Medium (DMEM) (Merck), containing 10% fetal bovine serum (FBS) and 1% penicillin / streptomycin (Merck). HEK293T cells transfected with pB-TetRep were grown in DMEM supplemented with tetracycline-free fetal bovine serum (FBS-tet) and 1% penicillin / streptomycin. In cell lines with integrated pB-CuRep or pB-TetRep cassettes, 3 mg/ml of puromycin (Merck) was added to the media. Cumate (System Biosciences) at a concentration of 300 mg/ml or tetracycline (Merck) at 3 mg/ml induced the expression of inserted cDNA. HEK293-TREx cells were cultured in DMEM with 10% fetal bovine serum tetracycline-free (FBS-tet) (Biosera), 1% Zell-Shield (Minerva Biolabs), and 5 mg/ml blasticidin. Tetracycline at a concentration of 3 mg/ml induced the expression of inserted cDNA. In cell lines expressing metalloproteins like hSOD1 and hCAII, 10  $\mu$ M ZnSO<sub>4</sub> (Sigma Aldrich) was added to the media upon induction of gene expression. For uniform <sup>15</sup>N labeling, <sup>15</sup>N labeled BioExpress6000 medium (CIL) was used instead of regular DMEM at the time of tetracycline induction (48 h before in-cell NMR measurement).

The HEK293-TREx and MCF7<sup>pKrox24DsRED</sup> cell lines were used to prepare an in-cell NMR sample of a 3D spheroid culture system consisting of two different cell lines. The MCF7 cell line bears pKrox24(MapErk)DsRED reporter<sup>37</sup> (Addgene #200114) integrated into the genome using piggyBac transposase<sup>38</sup>. The MCF7<sup>pKrox24DsRED</sup> cells respond to treatment with recombinant FGF2 (RnD Systems) by inducing the expression of destabilized red fluorescence protein (DsRED). The MCF7<sup>pKrox24DsRED</sup> cells were cultivated in DMEM containing 20% FBS and 1% penicillin/streptomycin. FGF2 (20 ng/ml; RnD Systems #233-FB-025) and heparin (1  $\mu$ g/ml; Merck Millipore #2106-10VL) were added to the media 24 h before the in-cell NMR experiment.

### Cell transfection and stable cell line generation

pB-CuRep and pB-Transp were co-transfected into HEK293T cells with FuGene HD Transfection Reagent (Promega). pB-TetRep and pB-Transp were co-transfected in the same manner into HEK293T and HEK293-TREx. The puromycin was added to the media 24 h after transfection to select efficiently transfected cells. Several polyclonal cell lines (HEK293T<sup>CuR-hSOD1/Poly</sup>, HEK293T<sup>TR-hSOD1/Poly</sup>, HEK293-TREx<sup>TR-hSOD1/Poly</sup>, HEK293-TREx<sup>TR-TTHA/Poly</sup>, HEK293-TREx<sup>TR-hCAII/Poly</sup>) were obtained after the selection. The addition of cumate or tetracycline induced the expression of the inserted gene. The intensity of the GFP signal (GFP reporter is co-expressed after tetracycline induction via an IRES element) was analyzed by FCM and fluorescent microscopy 48 h after the induction. The polyclonal cell lines (HEK293-TREx<sup>TR-hSOD1/Poly</sup>, HEK293-TREx<sup>TR-TTHA/Poly</sup>, HEK293-TREx<sup>TR-hCAII/Poly</sup>) generated monoclonal lines. Monoclonal cell lines (HEK293-TREx<sup>TR-hSOD1/Mono</sup>, HEK293-TREx<sup>TR-TTHA/Mono</sup>, HEK293-TREx<sup>TR-hCAII/Mono</sup>) were obtained by separation of 5% of the cells with the highest GFP signal on FACSaria Fusion cell sorter (see below). The intensity of GFP fluorescence of individual clones was analyzed 48 h after tetracycline induction by BD FACSVers flow cytometer, and the quantity of expressed proteins in the polyclonal and monoclonal cell lines was analyzed by Coomassie-stained SDS-PAGE, Western blot and microscopy (see below). Polyethylenimine (PEI) transfection was employed to transfect HEK293T cells with EGFP N1 (Clontech) or TTHA flag-tag (in pHL-sec) plasmid following a protocol by Banci et al.<sup>20</sup>.

### in-cell NMR sample preparation from stable cell lines

To express the protein of interest for NMR spectra acquisition, monoclonal cell lines (HEK293-TREx<sup>TR-hSOD1/Mono</sup>, HEK293-TREx<sup>TR-TTHA/Mono</sup>, HEK293-TREx<sup>TR-hCAII/Mono</sup>) were treated with 3  $\mu$ g/ml tetracycline 48 h before collecting and loading into the bioreactor.

### Cell synchronization in G1/S phase

HEK293-TREx<sup>TR-TTHA/Mono</sup> or HEK293-TREx<sup>TR-hCAII/Mono</sup> cells with ~40% confluency were treated with tetracycline (3  $\mu$ g/ml of media) 48 h before the in-cell NMR experiment. About 33 h later, the mimosine (Sigma Aldrich) was added to the media, and cells were incubated in 300  $\mu$ M mimosine for 14 h. After this, cells were harvested and loaded into the bioreactor (see below). Approximately 6 tissue culture flasks 75 cm<sup>2</sup> (TPP Techno Plastic Products AG) were needed to obtain ~400  $\mu$ l of the G1/S cellular slurry. The bioreactor medium was supplemented with 300  $\mu$ M mimosine to keep cells synchronized for 9 h. A small fraction of the cells was stored for further analysis of cell viability as a synchronization control.

### Cell synchronization in the G2/M phase

The initial steps of the G2/M synchronization were the same as in the G1/S synchronization. 24 h after tetracycline induction, the RO3306 (Sigma Aldrich) was added to the media and HEK293-TREx<sup>TR-TTHA/Mono</sup> or HEK293-TREx<sup>TR-hCAII/Mono</sup> cells were incubated in 9  $\mu$ M RO3306 for 24 h. After this, cells were harvested and loaded into the bioreactor. Approximately 6 tissue culture flasks 75 cm<sup>2</sup> (TPP Techno Plastic Products AG) were needed to obtain ~400  $\mu$ l of the cellular slurry. The bioreactor medium was supplemented with nocodazole (Sigma Aldrich) (300 ng/ml) to protect cells from escaping mitosis for 9 h. A small fraction of the cells was stored for further analysis of cell viability and synchronization control.

### Spheroid preparation

Spheroids for in-cell NMR were prepared using Elplasia plates (Corning®). Cells HEK293-TREx<sup>TR-TTHA/Mono</sup> and HEK293-TREx<sup>TR-hCAII/Mono</sup> cells were collected, washed with DPBS filtered on Cell Strainer 40 mm (VWR-Avantor), and counted in the Burk chamber. The cells were collected by centrifugation and resuspended in (isotopically <sup>15</sup>N-labeled) media supplemented with tetracycline and other compounds (see above). About 3.5  $\times$  10<sup>7</sup> cells were loaded on one Elplasia 6-well plate, pre-wetted with media-containing tetracycline. Spheroids were collected after 48 h of

incubation, and ~350  $\mu\text{l}$  of the spheroid pellet was used for the in-cell NMR sample.

### NMR bioreactor setup

The cell / spheroid pellet was mixed with 2% SeaPrep® agarose (Lonza) in DMEM at 37 °C in a v:v ratio of 1:1 (HEK293-Trex cells: agarose) or 2:3:5 v:v:v (spheroids: MCF7-pKrox24<sup>DSRED</sup> cells: agarose) in the case of preparation of an in-cell NMR sample of a 3D spheroid culture system consisting of two different cell lines. A PEEK capillary with a 0.75 mm inner diameter (or 1 mm inner diameter when preparing a sample from spheroids or spheroids/cell mixture) was filled with the mixture of agarose and cells/spheroid using a 1 ml syringe connected via a Luer adapter. The sample was incubated on ice for 10 min to solidify. A thread of the gel was then pushed with a syringe from the capillary into a 5 mm screw-cap NMR tube filled with bioreactor media: DMEM without NaHCO<sub>3</sub> (Sigma-Aldrich), 10% D<sub>2</sub>O (Eurisotop), 70 mM HEPES (Sigma-Aldrich), ZellShield, supplemented with 10  $\mu\text{M}$  ZnSO<sub>4</sub> when studying zinc containing metalloproteins and 100  $\mu\text{M}$  methazolamide (MZA) as a ligand for carbonic anhydrase II (CAII). The NMR cuvette with the sample was connected to a tubing system, ensuring media flow. The flow of the bioreactor medium was driven by an HPLC pump (ECP2010, ECOM, Czech Republic) from a reservoir incubated in a water bath at 37 °C through a vacuum degassing system (DG 4014, ECOM, Czech Republic) to the bottom of the NMR cuvette via a glass capillary connected to the inlet tubing. The fresh medium flowed through the sample, displacing the nutrient-depleted medium drained via the outlet tubing connected to an orifice in the cuvette lid. The flow rate was set to 50  $\mu\text{l}/\text{min}$ .

### In-cell NMR spectroscopy

In-cell 1D <sup>1</sup>H NMR spectra and 2D <sup>1</sup>H - <sup>15</sup>N NMR spectra were recorded on a Bruker Avance NEO 950 MHz NMR spectrometer (Bruker Corporation, Billerica, MA, USA) equipped with a TCI CryoProbe. A JR-echo (1-1 echo) pulse sequence<sup>39</sup> with zero excitation set to the resonance of water and the excitation maximum set to 13 ppm was used to acquire 1D <sup>1</sup>H in-cell NMR spectra. Spectra were processed by the exponential apodization function and baseline corrected. 2D <sup>1</sup>H - <sup>15</sup>N SOFAST-HMQC (Bruker pulse sequence sfhmqcf3gpph) spectra were recorded with frequency offsets of 4.7p.p.m. (<sup>1</sup>H) and 118.0 p.p.m. (<sup>15</sup>N), spectral windows of 16.5p.p.m. (<sup>1</sup>H) and 50p.p.m. (<sup>15</sup>N), acquisition times of 65.5 ms (<sup>1</sup>H) and 13.3 ms (<sup>15</sup>N) and an interscan delay of 0.15 s, using the shaped pulses Pc9\_4\_120.1000 and Rsnob.1000 for selective <sup>1</sup>H inversion and refocusing, respectively. Automatic (standard) procedures for tuning/matching (atma), shimming (topshim), and pulse calibration (pulsecal) were used with all samples. 1024 and 100 initial scans were typically employed to acquire 1D (~35 min) and 2D (~50 min) spectra. Both 1D and 2D spectra were recorded in a series and added up as necessary to obtain spectra with a sufficient signal-to-noise ratio. The bioreactor measurements typically required four to six times more experimental time than that required to measure spectra on pelleted cells. The obtained spectra were processed by an exponential apodization function with the line-broadening parameter (LB) set to 10. The NMR spectra were processed and analyzed using Bruker Topspin 4.0 (Bruker Corporation, Billerica, MA, USA) and MNova v14.2.1 software (Mestrelab Research, Spain). All NMR spectra were measured at 37 °C using a bioreactor unless indicated otherwise.

### Flow cytometry and sorting

FCM analysis of viability and GFP fluorescence: Roughly 10<sup>5</sup> cells were resuspended in 200  $\mu\text{l}$  of DPBS buffer (Sigma-Aldrich). To distinguish the apoptotic, dead cells or cells with compromised membrane integrity from the living cells, the sample was stained with 1  $\mu\text{l}$  (1 mg/ml) of propidium iodide (PI) (Exbio). The total amount of 10<sup>4</sup> cells was analyzed by a BD FACSVerser flow cytometer using BD FACSuite software V1.0.6 (BD Biosciences, USA). To detect the GFP fluorescence in the cells after tetracycline induction, the excitation and emission wavelengths were 488 nm and 527/32 nm, respectively.

PI was excited at 488 nm to evaluate the cell viability, and the emission was detected at 700/54 nm.

Analyzing of DNA content in fixed cells stained with PI: The amount of 8 × 10<sup>6</sup> cells were fixed with ice-cold 70% (v/v) ethanol, incubated overnight at -20 °C, washed twice with ice-cold DPBS, and incubated 45 min at 37 °C in DPBS containing freshly added PI (50  $\mu\text{g}/\text{ml}$ ) and RNase A (200  $\mu\text{g}/\text{ml}$ ; Qiagen, 19101). Directly before FACS analysis, 5 mM EDTA was added into the suspension and cells were filtered by Non-sterile CellTrics™ filters with 5  $\mu\text{m}$  pores (Sysmex). For FACS analysis, the excitation wavelength was set at 488 nm for PI to visualize the DNA content. The PI emission was detected at 700/54 nm. FACS sorting – generation of monoclonal cell lines: The polyclonal cell lines (HEK293-Trex<sup>TR-hSOD1</sup>, HEK293-Trex<sup>TR-TTHA</sup>, HEK293-Trex<sup>TR-hCAII</sup>) collected 48 h after tetracycline addition were resuspended in FACS buffer (PBS, 2% FBS, 5 mM EDTA) and sorted by FACSAria Fusion cell sorter using BD FACSDiva software V8.0.1 (BD Biosciences, USA). To obtain monoclonal cell lines (HEK293-Trex<sup>TR-hSOD1/Mono</sup>, HEK293-Trex<sup>TR-TTHA/Mono</sup>, HEK293-Trex<sup>TR-hCAII/Mono</sup>), approximately 5% of the cells with the highest GFP signal were sorted into the 96-well plate by one cell per 1 well. Figure S8 exemplifies the employed gating strategy.

### SDS PAGE

SDS-PAGE was performed on Mini Protean Vertical Electrophoresis (BioRad). Cells or spheroids from monoclonal cell lines were collected 48 h after tetracycline addition and lysed in RIPA lysis buffer (50 mM Tris-HCl, 150 mM NaCl, 1% NP-40, 0.5% sodium deoxycholate 0.1% SDS) supplemented with cComplete™ EDTA-free Protease Inhibitor Cocktail (Roche). Total protein concentration was determined by Bradford assay (BioRad). Equal amounts of total proteins were run on 16% Tris-Tricine SDS-PAGE in Tris-Tricine running buffer. Afterward, the gels were stained with Coomassie blue solution.

### Western blot

Cells from monoclonal cell lines were collected 48 h after tetracycline addition, counted, and lysed in RIPA lysis buffer (50 mM Tris-HCl, 150 mM NaCl, 1% NP-40, 0.5% sodium deoxycholate 0.1% SDS) supplemented with cComplete™ EDTA-free Protease Inhibitor Cocktail (Roche). The total protein concentration was estimated using Bradford Protein Assay (BIO-RAD). The flag-tagged TTHA recombinant protein of known concentration was used as a standard to estimate the concentration of flag-tagged proteins overexpressed in monoclonal cell lines.

Samples of lysates and recombinant protein were loaded on gradient 4–15% precast polyacrylamide gel (BIO-RAD) and separated by electrophoresis in 1 x TBE running buffer (89 mM Tris, 89 mM boric acid, 2 mM EDTA). Proteins were transferred from the gel to the PVDF membrane (Immun-Blot®PVDF Membrane, BIO-RAD) using semi-dry blotting in 1 x transfer buffer (48 mM Tris, 39 mM glycine, 20% methanol, pH 8.5) at a constant current 0.8 mA/cm<sup>2</sup> for 90 min. (Trans-Blot® Turbo™ Transfer System, BIO-RAD, USA). Upon membrane blocking with 5% skim milk and 5% BSA in TBST (150 mM NaCl, 50 mM TRIS-HCl, pH 7.8, 1 M EDTA, 0.1% Tween-20), proteins on the membrane were detected by immunostaining with the primary antibody (Anti-FLAG, clone M2, cat.no. F1804; MERCK) in the blocking solution, followed by washing in TBST and incubation with horseradish peroxidase-conjugated secondary antibody (goat anti-mouse antibody, cat.no. 115-035-003; Jackson Immuno Research) in the blocking solution. After washing with TBST, protein signals were visualized by incubation of the membrane in ECL substrate (Clarity™ Western ECL Substrate, BIO-RAD), and chemiluminescence was detected with Odyssey®Fc Imaging System (LI-COR).

### Microscopy

The microscopy images of the living cells monitoring GFP signal intensity after tetracycline/cumate treatment were obtained using a CELEROMICS optical system connected to an inverted fluorescence microscope NIB-100F (Novel Optics). Light transmission images were obtained with objectives PLAN PH 4x/0.1 and PLAN PH 10x/0.25. The objective PLAN PH 4x/0.1

and PLAN F 10x/0.3 were used for fluorescence mode. GFP signal was analyzed with an excitation wavelength of 460–490 nm and detected at emission wavelengths over 520 nm. The excitation wavelength for DsRed was set to 480–550 nm, and the emission was detected at over 590 nm. The images were collected and analyzed using CELEROMICS software. For the immunofluorescence analysis, the monoclonal cells were plated on 0.02% gelatine-coated coverslips in 24 well plates and treated with tetracycline. 48 h after tetracycline addition, coverslips were washed once with DPBS (Sigma Aldrich) and fixed in a 4% paraformaldehyde (ChemCruz) and 0.02% sucrose (AppliChem) DPBS solution for 10 min at room temperature. The cells were washed twice with DPBS and incubated overnight at -20 °C with ice-cold methanol. Samples were washed with DPBS and blocked for 30 min with 3% BSA and 0.05% Tween20 in DPBS (PBS-BSA-T) solution for 30 min at room temperature and incubated over-night at 4 °C with mouse monoclonal anti-flag antibody (Anti-FLAG, clone M2, dilution 1:500 cat.no. F1804; Sigma Aldrich.) in PBS-BSA-T solution and washed three times with DPBS - 0.05% Tween20 (PBS-T) solution. Subsequently, the samples were incubated with goat anti-mouse Alexa 594 conjugated antibody (dilution 1:500, cat. no.115-585-146; Jackson Immune Research) PBS-BSA-T solution. Cells were washed three times with PBS-T solution, and coverslips were dried and mounted with VECTASHIELD® PLUS Antifade Mounting Medium with DAPI (H-2000) (Vector Laboratories). The microscopy images were obtained using a Zeiss LSM 800 confocal microscope with an Apochromat 63x / 1.40 OIL objective. The GFP signal was analyzed with an excitation wavelength of 488 nm, for the GFP signal was detected at emission wavelengths of 502–558 nm. The excitation wavelength for DAPI was set to 405 nm, and the emission was detected at 400–488 nm. The excitation wavelength for Alexa 594 was set to 594 nm, and the emission was detected at 604–700 nm. The images were collected and analyzed in ZEN Blue 2.6 and 3.1 software. The microscopy images of the samples mimicking the tissue (a small fraction of agarose throat containing mixture HEK293-T<sup>Rex<sup>TR-hCALI</sup></sup> spheroids and MCF7pKrox24<sup>DsRED</sup> cells) were obtained using a Zeiss LSM 700 Axio scanning confocal microscope with a N-Achroplan 10 x /0.3 Wdip objective. GFP signal was analyzed with an excitation wavelength of 488 nm and detected at 300–550 nm emission wavelengths. The excitation wavelength for DsRED was set to 555 nm, and the emission was detected at 560–800 nm. The images were collected and analyzed in ZEN Blue 2.6 and 3.1 software.

### Reporting summary

Further information on research design is available in the Nature Portfolio Reporting Summary linked to this article.

### Data availability

Plasmids (and their maps) generated in this study are available in the Addgene plasmid repository under the ID numbers 232477, 232478, 232479, 232480, 23248, and 232781. All data generated in this study are available in the Article and Supplementary Information section. The raw in-cell NMR data generated in this study have been deposited in the public data repository<sup>40</sup>.

Received: 27 June 2024; Accepted: 27 January 2025;

Published online: 07 February 2025

### References

- Theillet, F.-X. et al. Physicochemical properties of cells and their effects on intrinsically disordered proteins (IDPs). *Chem. Rev.* **114**, 6661–6714 (2014).
- Cheng, K. et al. Crowding and confinement can oppositely affect protein stability. *ChemPhysChem* **19**, 3350–3355 (2018).
- Stewart, C. J., Olgenblum, G. I., Propst, A., Harries, D. & Pielak, G. J. Resolving the enthalpy of protein stabilization by macromolecular crowding. *Prot. Sci.* **32**, e4573 (2023).
- Inomata, K. et al. High-resolution multi-dimensional NMR spectroscopy of proteins in human cells. *Nature* **458**, 106–109 (2009).
- Takaoka, Y. et al. Quantitative comparison of protein dynamics in live cells and in vitro by in-cell <sup>19</sup>F-NMR. *Chem. Commun.* **49**, 2801 (2013).
- Theillet, F.-X. et al. Structural disorder of monomeric α-synuclein persists in mammalian cells. *Nature* **530**, 45–50 (2016).
- Tanaka, T. et al. High-resolution protein 3D structure determination in living Eukaryotic cells. *Angew. Chem. Int. Ed. Engl.* **58**, 7284–7288 (2019).
- Luchinat, E. et al. Intracellular binding/unbinding kinetics of approved drugs to carbonic anhydrase II observed by in-cell NMR. *ACS Chem. Biol.* **15**, 2792–2800 (2020).
- Plitzko, J. M., Schuler, B. & Selenko, P. Structural biology outside the box — inside the cell. *Curr. Opin. Struct. Biol.* **46**, 110–121 (2017).
- Theillet, F.-X. In-cell structural biology by NMR: the benefits of the atomic scale. *Chem. Rev.* **122**, 9497–9570 (2022).
- Theillet, F.-X. & Luchinat, E. In-cell NMR: why and how? *Prog. Nucl. Magn. Reson. Spectrosc.* **132–133**, 1–112 (2022).
- Ogino, S. et al. Observation of NMR signals from proteins introduced into living mammalian cells by reversible membrane permeabilization using a pore-forming toxin, streptolysin O. *J. Am. Chem. Soc.* **131**, 10834–10835 (2009).
- Sciolino, N. et al. Microfluidics delivery of DARPP-32 into HeLa cells maintains viability for in-cell NMR spectroscopy. *Commun. Biol.* **5**, 451 (2022).
- Luchinat, E. & Banci, L. In-cell NMR in human cells: direct protein expression allows structural studies of protein folding and maturation. *Acc. Chem. Res.* **51**, 1550–1557 (2018).
- Odermatt, P. D. et al. Variations of intracellular density during the cell cycle arise from tip-growth regulation in fission yeast. *eLife* **10**, e64901 (2021).
- Spear, J. S. & White, K. A. Single-cell intracellular pH dynamics regulate the cell cycle by timing the G1 exit and G2 transition. *J. Cell Sci.* **136**, jcs260458 (2023).
- Wu, W. et al. Measuring single-cell density with high throughput enables dynamic profiling of immune cell and drug response from patient samples. *bioRxiv* <https://doi.org/10.1101/2024.04.25.591092> (2024).
- Li, C. et al. Protein 19 F NMR in *Escherichia Coli*. *J. Am. Chem. Soc.* **132**, 321–327 (2010).
- DeMott, C. M., Majumder, S., Burz, D. S., Reverdatto, S. & Shekhtman, A. Ribosome mediated quinary interactions modulate in-cell protein activities. *Biochemistry* **56**, 4117–4126 (2017).
- Banci, L. et al. Atomic-resolution monitoring of protein maturation in live human cells by NMR. *Nat. Chem. Biol.* **9**, 297–299 (2013).
- Krude, T. Mimosine arrests proliferating human cells before onset of DNA replication in a dose-dependent manner. *Exp. Cell Res.* **247**, 148–159 (1999).
- Watson, P. A., Hanauske-Abel, H. H., Flint, A. & Lalande, M. Mimosine reversibly arrests cell cycle progression at the G1–S phase border. *Cytometry* **12**, 242–246 (1991).
- Vassilev, L. T. et al. Selective small-molecule inhibitor reveals critical mitotic functions of human CDK1. *Proc. Natl. Acad. Sci. USA.* **103**, 10660–10665 (2006).
- Kubo, S. et al. A gel-encapsulated bioreactor system for NMR studies of protein–protein interactions in living mammalian cells. *Angew. Chem. Int. Ed. Engl.* **52**, 1208–1211 (2013).
- Luchinat, E. et al. Drug screening in human cells by NMR spectroscopy allows the early assessment of drug potency. *Angew. Chem. Int. Ed. Engl.* **59**, 6535–6539 (2020).
- Fennema, E., Rivron, N., Rouwkema, J., Van Blitterswijk, C. & De Boer, J. Spheroid culture as a tool for creating 3D complex tissues. *Trends Biotechnol.* **31**, 108–115 (2013).



27. Levinger, I., Ventura, Y. & Vago, R. Life is three dimensional—as in vitro cancer cultures should be. *Adv. Cancer Res.* **121**, 383–414 (2014).
  28. Huguet, E. L., McMahon, J. A., McMahon, A. P., Bicknell, R. & Harris, A. L. Differential expression of human Wnt genes 2, 3, 4, and 7B in human breast cell lines and normal and disease states of human breast tissue. *Cancer Res.* **54**, 2615–2621 (1994).
  29. Pham, L. B. T. et al. Direct Expression of Fluorinated Proteins in Human Cells for <sup>19</sup>F In-Cell NMR Spectroscopy. *J. Am. Chem. Soc.* **145**, 1389–1399 (2023).
  30. Víšková, P. et al. In-cell NMR suggests that DNA i-motif levels are strongly depleted in living human cells. *Nat. Commun.* **15**, 1992 (2024).
  31. Narasimhan, S. et al. DNP-supported solid-state NMR spectroscopy of proteins inside mammalian cells. *Angew. Chem. Int. Ed. Engl.* **58**, 12969–12973 (2019).
  32. Kadavath, H., Cecilia Prymaczok, N., Eichmann, C., Riek, R. & Gerez, J. A. Multi-dimensional structure and dynamics landscape of proteins in mammalian cells revealed by in-cell NMR. *Angew. Chem. Int. Ed. Engl.* **62**, e202213976 (2023).
  33. Gerez, J. A. et al. Protein structure determination in human cells by in-cell NMR and a reporter system to optimize protein delivery or transexpression. *Commun. Biol.* **5**, 1322 (2022).
  34. Mao, G. et al. DNA context and promoter activity affect gene expression in lentiviral vectors. *Acta Biomed.* **79**, 192–196 (2008).
  35. Krafcikova, M. et al. Monitoring DNA-Ligand Interactions in Living Human Cells Using NMR Spectroscopy. *J. Am. Chem. Soc.* **141**, 13281–13285 (2019).
  36. Schwalbe, H. et al. The future of integrated structural biology. *Structure* **32**, 1563–1580 (2024).
  37. Gudernova, I. et al. One reporter for in-cell activity profiling of majority of protein kinase oncogenes. *eLife* **6**, e21536 (2017).
  38. Weissová, K. et al. LuminoCell: A versatile and affordable platform for real-time monitoring of luciferase-based reporters. *Life Sci. Alliance* **5**, e202201421 (2022).
  39. Sklenář, V. & Bax, A. Spin-echo water suppression for the generation of pure-phase two-dimensional NMR spectra. *J. Magn. Reson.* **74**, 469–479 (1987).
  40. Rynes, J., Istvankova, E., Foldynova-Trantirkova, S. & Trantirek, L. Protein structure and interactions elucidated with in-cell NMR for different cell cycle phases and in 3D human tissue models. *figshare*. <https://doi.org/10.6084/m9.figshare.28266740.v1> (2025).
- National Institute for Cancer Research (Programme EXCELES, ID Project No. LX22NPO5102) to P.K. and S.F.T. - Funded by the European Union - Next Generation EU, and Ministry of Education, Youth, and Sports of the Czech Republic (LUAUS23295) to P.K. G.R. was supported by a post-doctoral fellowship of the Internal Grant Agency of the Faculty of Medicine, Masaryk University. P.K. has been supported by Praemium Academiae of the Czech Academy of Sciences. B.F. was supported by the Agency for Healthcare Research of the Czech Republic (NU21-06-00512).

### Author contributions

L.T., S.F.T., E.L., L.Bar., L.Ban., L.M., and P.K. designed research; J.R., E.I., M.D.K., K.K., T.L., G.R.L., and S.F.T. performed experiments; P.K. contributed MCF7<sup>pKrox24DsRED</sup> cells; B.F. contributed reagents and protocols for transposon integration; L.M. contributed reagents and protocols for cell cycle synchronization; L.T., S.F.T., J.R., E.I., E.L., and M.D.K. analyzed data; L.T., S.F.T., and J.R. wrote the manuscript; all authors contributed to the manuscript editing.

### Competing interests

The authors declare no competing interests.

### Additional information

**Supplementary information** The online version contains supplementary material available at <https://doi.org/10.1038/s42003-025-07607-w>.

**Correspondence** and requests for materials should be addressed to Silvie Foldynova-Trantirkova or Lukas Trantirek.

**Peer review information** *Communications Biology* thanks the anonymous reviewers for their contribution to the peer review of this work. Primary Handling Editors: Luciano Abriata and Laura Rodríguez Pérez.

**Reprints and permissions information** is available at <http://www.nature.com/reprints>

**Publisher's note** Springer Nature remains neutral with regard to jurisdictional claims in published maps and institutional affiliations.

**Open Access** This article is licensed under a Creative Commons Attribution-NonCommercial-NoDerivatives 4.0 International License, which permits any non-commercial use, sharing, distribution and reproduction in any medium or format, as long as you give appropriate credit to the original author(s) and the source, provide a link to the Creative Commons licence, and indicate if you modified the licensed material. You do not have permission under this licence to share adapted material derived from this article or parts of it. The images or other third party material in this article are included in the article's Creative Commons licence, unless indicated otherwise in a credit line to the material. If material is not included in the article's Creative Commons licence and your intended use is not permitted by statutory regulation or exceeds the permitted use, you will need to obtain permission directly from the copyright holder. To view a copy of this licence, visit <http://creativecommons.org/licenses/by-nc-nd/4.0/>.

© The Author(s) 2025

### Acknowledgements

The authors thank Katerina Cermakova for assistance with WB analysis and acknowledge the institutional projects enabling access to research infrastructure: iNEXT-Discovery [871037] financed by the Horizon 2020 program of the European Commission, Josef Dadok National NMR Centre of CIISB, Instruct-CZ Centre, supported by MEYS CR (LM2023042) and European Regional Development Fund-Project „UP CIISB“ (No. CZ.02.1.01/0.0/0.0/18\_046/0015974), core facility CELLIM supported by MEYS CR (LM2023050 Czech-Biolmaging), and the Flow Cytometry Laboratory at CEITEC MU supported by the EATRIS-ERIC-CZ research infrastructure (LM2023053 funded by MEYS CR). This research was supported by grants from the Czech Science Foundation (GX19-26041X to L.T. and GF21-26400K to P.K.); Instruct-ERIC, a Landmark ESFRI project, and specifically by the CERM/CIRMMP Italian Instruct Center to E.L., L.Barbieri and L.Banci,